

The aluminium(III) complex of hypocrellin B as a PDT photosensitizer

Jianghua Ma, Jingquan Zhao* and Lijin Jiang

Center for Molecular Science, Institute of Chemistry, The Chinese Academy of Sciences, Beijing, 100080, China.

Received (in Montpellier, France) 2nd March 2001, Accepted 2nd April 2001

First published as an Advance Article on the web 16th May 2001

The complex of hypocrellin B (HB) with aluminium was synthesized to improve the water solubility and red absorption of the parent pigment. The complexation of HB with Al^{3+} resulted in the formation of a complex with 1 : 1 $\text{Al(III)} : \text{HB}$ stoichiometry (Al^{3+} -HB) measured by molar ratio and continuous variation methods, respectively. The structure of this complex has been characterized by UV-Vis, IR, ^1H NMR and elemental analysis data. Compared with HB, the complex possesses excellent solubility in water; in addition, the absorption wavelength of Al^{3+} -HB shifts bathochromically into the phototherapeutic window (600–900 nm). The generation of active oxygen species, including the superoxide radical anion ($\text{O}_2^{\cdot-}$) and singlet oxygen ($^1\text{O}_2$), by Al^{3+} -HB photosensitization was observed. The efficiency of $\text{O}_2^{\cdot-}$ generation by Al^{3+} -HB was twice as much as that of HB. Under our experimental conditions, the rate of $\text{O}_2^{\cdot-}$ generation by Al^{3+} -HB was about $2.3 \mu\text{M min}^{-1}$ measured by the cytochrome c reduction method using 578 nm light. The quantum yield of singlet oxygen ($^1\text{O}_2$) was 0.23 in DMSO determined by the 9,10-DPA (diphenylanthracene) photobleaching experiments. These results suggest that the new complex possesses an enhanced type I process but a decreased type II process as compared with hypocrellin B.

Introduction

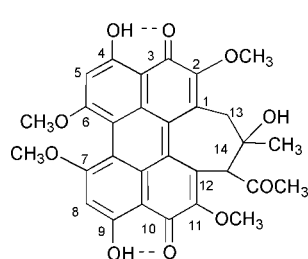
Photodynamic therapy (PDT), as a multimodality treatment procedure, requires both a selective photosensitizer and a powerful light source that matches the absorption spectrum of the photosensitizer. Through the excitation of photosensitizers to excited singlet and/or triplet states, the tumor is destroyed, either by singlet oxygen species (type II mechanism) or by radical products (type I mechanism).¹ PDT offers a unique alternative treatment for malignant tumors resistant to conventional therapies, with the potential for selective destruction of malignant cells. However, in practice, the advance of this therapeutic modality has been hampered by the undesirable side effects of some photosensitizers, such as those of the porphyrin family. This has prompted intense research on second-generation photosensitizers, of which hypocrellin B is an example.

Hypocrellin B (**2**) is a new type of photosensitive pigment and medicine, deriving its name from the natural fungus *Hypocrella bambusae* (B et Br) sacc growing abundantly in China.^{2–5} *In vivo* studies have indicated that the tissue dis-

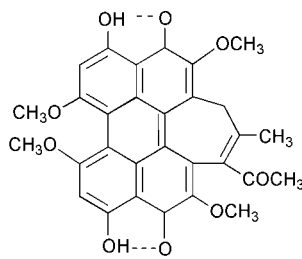
tribution pattern of hypocrellin B is similar to that of Photofrin II, but with faster kinetics.^{6–10} A significant finding was the rapid clearance rate of hypocrellin B from plasma and its maximum incorporation into murine tumor within 2 h of intravenous administration. This might be the reason why hypocrellin B generally causes much less delayed skin photosensitization in both animals and humans compared to porphyrins such as Photofrin II.

However, hypocrellin B is insoluble in water and, as in the case of Photofrin II, does not exhibit strong absorption at wavelengths longer than 600 nm. These disadvantages hamper investigations into its biological consequences and limit its clinical PDT application.

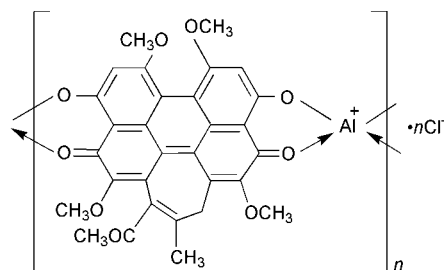
To improve the water solubility and red absorption of hypocrellin B, we have recently synthesized a series of HB derivatives.^{11–19} Among the derivatives, the metal complexes are the most attractive due to their easy synthesis, high yields and good photodynamic efficiencies.^{18,19} Preliminary studies indicated that the complexes of hypocrellin A (HA, **1**) with group IIIA metal ions, such as Al^{3+} or B^{3+} , are very stable and have good water-solubility compared to HA complexes with group IIA metal ions.²⁰ However, under some experimental conditions, HA is unstable and may be transformed into HB, which would produce many more by-products during the reaction processes.²¹ Moreover, HB can be



1



2



3

obtained almost quantitatively from the transformation of HA.²² There have been some investigations on the metal ion-complexed derivatives of hypocrellins; however, systematic and, especially, quantitative studies on the photodynamic actions of these complexes have not yet been performed. In this work, we chose HB as the model compound and synthesized the complex of HB with Al³⁺. Full experimental data on the synthesis and characterization of Al³⁺-HB (**3**) is reported. In addition, we investigated the generation of superoxide radical anions (O₂^{•-}) and singlet oxygen (¹O₂) through photosensitization of this new material using electron paramagnetic resonance (EPR) and spectrophotometric methods. To quantify the formation of O₂^{•-} during Al³⁺-HB-mediated photosensitization, we have utilized the cytochrome c reduction method. The quantum yield of ¹O₂ generated by Al³⁺-HB was also determined.

Experimental

Chemicals

Hypocrellin B was prepared as described previously.²² 5,5-Dimethyl-1-pyrroline-*N*-oxide (DMPO), 2,2,6,6-tetramethyl-4-piperidone (TEMP) and 9,10-diphenylanthracene (DPA) were purchased from Aldrich Chemical Company. Superoxide dismutase (SOD) and cytochrome c were purchased from Sigma Chemical Company. Reduced nicotinamide adenine dinucleotide (NADH) was obtained from Biochem. Technology Corporation, the Chinese Academy of Sciences. 1,4-Diazabicyclo[2.2.2]octane (DABCO) and dimethylsulfoxide (DMSO) were purchased from Merck Chemical Company. Anhydrous AlCl₃, sodium azide (NaN₃), deuterated solvents and other agents of analytical grades were purchased from Beijing Chemical Plant. The working stock solutions were prepared immediately before use.

Synthesis of the complex of HB with Al³⁺

AlCl₃ (100 mg) and HB (95 mg) were mixed and vigorously stirred in CHCl₃ (20 ml) for 5 min at rt in the dark. The mixture was filtered and the solvent evaporated from the filtrate under reduced pressure. The residue obtained was re-dissolved in deionized water and dialyzed against deionized water using a Spectrapor membrane with a molecular weight cut-off of 6000–8000. The low molecular weight components (<6000–8000) diffusive across the Spectrapor, while the higher molecular weight materials are left inside the dialysis bag. After dialysis, the retained solution was dried and the desired complex (dark-red, amorphous powder) was obtained (108 mg, yield: 91%) (Anal. calc. for Cl⁻·Al³⁺-HB (C₃₀H₂₂AlClO₉): C, 61.22; H, 3.74; O, 24.49; Cl, 5.95; Al, 4.60%. Found: C, 60.78; H, 3.87; O, 24.78; Cl, 5.93; Al, 4.64%).

Spectroscopic measurements

The UV-Vis absorption spectra were recorded on a Shimadzu UV-1601 spectrophotometer. Fluorescence spectra were

recorded on a Hitachi F-4500 fluorescence spectrophotometer. The fluorescence quantum yield was obtained by the relative method using HB in DMSO as a standard. The fluorescence quantum yield of HB was assumed to be 0.0058 and the excitation wavelength used was 570 nm.²³ In all cases, the absorbance values at the excitation wavelength were lower than 0.1 for a 1 cm pathlength. IR spectra were measured with a BIO-RAD FTS 165 grating spectrometer. ¹H NMR spectra were measured with a Varian XL-400 instrument (300 MHz). Elemental analyses (C, H, O) were performed on a Carlo Erba-1106 elemental analyzer. The percentage of chlorine was measured by the Hg titration method. The percentage of aluminium was measured on an IRIS Advantage ICP emission spectrophotometer.

Characterization of the Al³⁺-HB complex

The complexation of HB with increasing amounts of Al³⁺ can be recorded spectrophotometrically. The addition of Al³⁺ causes a bathochromic shift and an increase in the intensity of the absorption bands of HB (Fig. 1). The changes in the absorption spectra imply that a complex of HB with Al³⁺ is produced. When the concentration of Al³⁺ added to the solution reached 100 μM, which was equal to the initial HB concentration, the changes in the absorption spectra tended to tail off.

During complexation, a single group of isosbestic points at 315, 349, 384 and 462 nm was maintained within the spectral region (300–700 nm) under study, indicating that only one species is produced in the system. The absorption data for the Al³⁺-HB complex are shown in Table 1.

It may be observed that the absorption spectrum of the Al³⁺-HB complex is somewhat similar to that of the dianion of HB. Fig. 2 shows the absorption spectrum of HB in NaOH solution. This suggests that Al³⁺ bonds with the phenolic hydroxy oxygen and the carbonyl oxygen of HB, through removal of the phenolic hydroxy proton.

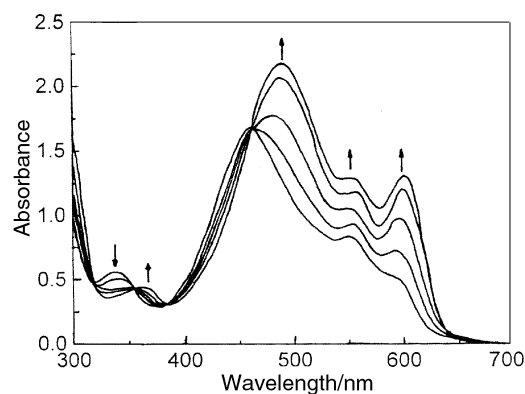


Fig. 1 Changes in the absorption spectrum of HB on addition of various amounts of Al³⁺ to an ethanol solution of HB (100 μM). [Al³⁺]/[HB] = 0, 0.2, 0.5, 1, 4. Arrows indicate the directions of change.

Table 1 Spectral parameters of HB and Al³⁺-HB complex

Compound	$\lambda_{\text{max}}^{\text{A}}/\text{nm}$ (DMSO)	$\lambda_{\text{max}}^{\text{F}}/\text{nm}$ (DMSO)	$\Phi_{\text{F}} \times 10^3$	$\delta_{\text{H}}[(\text{CD}_3)_2\text{SO}]$
2	468, 545, 590	618	5.8	16.27, 16.20 (2H, s); 6.65, 6.63 (2H, s); 4.11, 4.08, 4.07, 3.97 (12H, s); 3.94, 3.18 (2H, dd, $J = 11$ Hz); 2.28 (3H, s); 1.83 (3H, s)
3	503, 568, 614	621	2.3	6.75, 6.66 (2H, s); 4.18, 4.12, 4.09, 4.01 (12H, s); 3.98, 3.22 (2H, dd, $J = 11$ Hz); 2.35 (3H, s); 1.92 (3H, s)

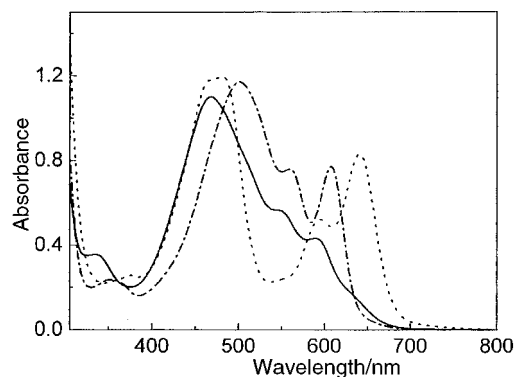


Fig. 2 Absorption spectra of HB and Al^{3+} -HB measured in NaOH and DMSO solution. (—) HB ($3.3 \times 10^{-5} \text{ mol L}^{-1}$) in DMSO, (···) HB ($3.3 \times 10^{-5} \text{ mol L}^{-1}$) in NaOH, (---) Al^{3+} -HB in DMSO (0.22 mg ml^{-1} ; $\leq 3.3 \times 10^{-5} \text{ mol L}^{-1}$).

The ^1H NMR and IR data also support this conclusion. The ^1H NMR data show that the signals of the two phenolic hydroxy groups of HB in $(\text{CD}_3)_2\text{SO}$ disappear on formation of the Al^{3+} -HB complex (Table 1). IR spectra were obtained using KBr discs of the solids. The characteristic absorption band of the quinonoid carbonyl group in HB (1612 cm^{-1}) shifts bathochromically to 1598 cm^{-1} on coordination of the carbonyl oxygen with Al^{3+} . The Al^{3+} -HB complex shows a strong absorption band at 1511 cm^{-1} and a broad absorption band around 600 cm^{-1} , which are the characteristic absorptions of the complexed ring and Al^{3+} -O band, respectively.^{24,25} These observations may be interpreted as evidence for the formation of a ring system with an aluminium heteroatom.

The ratio of Al^{3+} to HB in the Al^{3+} -HB complex was examined by molar ratio and continuous variation methods, which were established by Harvey and Manning.²⁶ For the molar ratio method we prepared a series of ethanol solutions with different concentrations of Al^{3+} , whilst keeping the concentration of HB ($47.3 \mu\text{M}$) constant. The formation of the Al^{3+} -HB complex was followed spectrophotometrically by detecting the increase in absorption at 600 nm where Al^{3+} and HB exhibit low absorption. As shown in Fig. 3, two straight lines with different slopes are observed. The extrapolated intersection occurs at the molar ratio of 1:1 for the two reactants in the complex. For the continuous variation method, the total concentration of Al^{3+} and HB was kept constant ($47.3 \mu\text{M}$) while the molar fractions of Al^{3+} and HB were continuously varied. The difference (Y) between the absorbance of the complex and that of the free HB was plotted against the molar fraction of Al^{3+} . As shown in Fig. 4, the maximum of Y occurs at an Al^{3+} molar fraction of 0.5,

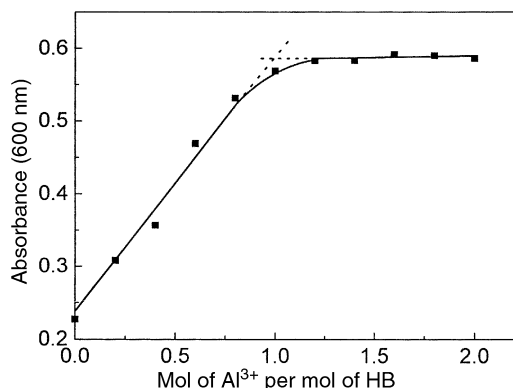


Fig. 3 Molar ratio plot for the Al^{3+} -HB complex in ethanol, obtained by plotting the absorbance at 600 nm as a function of the molar ratio of Al^{3+} to HB.

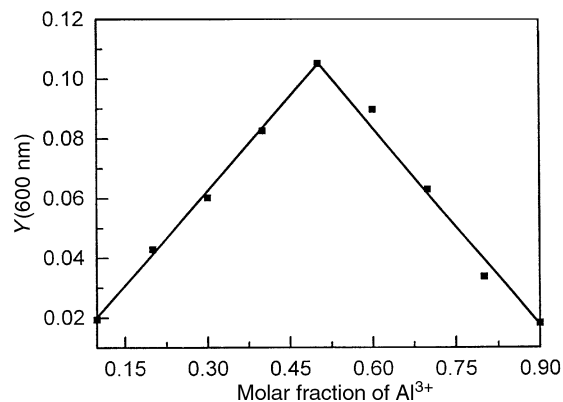


Fig. 4 Continuous variation plot for the Al^{3+} -HB complex in ethanol, obtained by plotting the absorbance at 600 nm with a correction made for uncoordinated HB absorption as a function of the molar fraction of Al^{3+} .

i.e. a molar ratio of 1:1 Al^{3+} to HB, corresponding to the ratio in the complex.

Thus, the molar ratio and continuous variation methods gave consistent results, *i.e.* HB forms a 1:1 complex with Al^{3+} .

Furthermore, the addition of appropriate counter-anions in the Al^{3+} -HB water solution, such as SO_3^{2-} , led to the precipitation of the corresponding salt of the complex and the precipitate re-dissolved in water upon addition of hydrochloric acid, which confirms the cationic nature of this complex. The elemental analytical data for the complex also indicate a 1:1 metal-ligand stoichiometry in the solid and that the counter-ion is chloride. The addition of AgNO_3 to the Al^{3+} -HB water solution led to the precipitation of AgCl , which further confirms that Cl^- is the counter-ion in the complex. Therefore, we propose a polymeric cationic structure (3), similar to that of Al^{3+} -HA.²⁰

EPR measurements

The EPR measurements were performed using an aqueous flat cell at 9.80 GHz in a Bruker ESP 300E spectrometer at room temperature. Photoinduced EPR spectra were measured from samples ($40 \mu\text{l}$) injected into quartz capillaries designed specially for EPR analysis. Samples were irradiated directly inside the microwave cavity of the spectrometer using a 532 nm YAG-900 Laser (Spectro-Physics, Mountain View, CA, USA) with an intensity of 100 mW cm^{-1} and a flux of 20 J cm^{-2} . EPR spectra were recorded and manipulated using an IBM/PC computer. The kinetics of spin adduct generation were studied by recording peak heights of the EPR spectra every 30 s . To make the production efficiencies of all spin adducts comparable, the concentrations of Al^{3+} -HB and HB were adjusted to keep the same optical density (OD) at 532 nm .

Determination of the quantum yield of $^1\text{O}_2$ generated by the DPA bleaching method

The photobleaching of 9,10-diphenylanthracene (DPA) was used to determine the quantum yields of $^1\text{O}_2$ generation.²⁷

The photo-oxidation of DPA sensitized by Al^{3+} -HB was carried out on a 'merry-go-round' apparatus, using a high-pressure mercury lamp (500 W) as the light source in combination with a 578 nm monochromatic filter. The reactions were followed spectrophotometrically by observing the decrease in the 374 nm absorption peak of DPA (where the photosensitizer used has the lowest absorption) as a function of irradiation time.

Reduction of cytochrome c

The generation of superoxide anion ($\text{O}_2^{\cdot-}$) was also detected by monitoring the SOD-inhibitable reduction of cytochrome c.^{28–33} The extent of cytochrome c reduction was monitored spectrophotometrically at 550 nm using a Shimadzu UV-1601 spectrophotometer before the irradiation (A_0) and after various irradiation times (A_t). The molar extinction coefficient is $0.89 \times 10^4 \text{ M}^{-1} \text{ cm}^{-1}$ for ferricytochrome c (CytFe^{3+}) and $2.94 \times 10^4 \text{ M}^{-1} \text{ cm}^{-1}$ for ferrocyanochrome c (CytFe^{2+}), respectively.^{28,30,33} Therefore the concentration of the reduced cytochrome c (CytFe^{2+}) can be determined from the formula $(A_t - A_0)/(2.05 \times 10^4)$ in units of mol per litre. A high-pressure mercury vapor lamp (500 W) in combination with a 578 nm monochromatic filter was used as the light source, as before.

Results and discussion

Al^{3+} -HB (3) is readily soluble in polar organic solvents and in water. With respect to HB, the absorption peaks in DMSO shifted bathochromically to 503, 568 and 614 nm. The fluorescence quantum yield of Al^{3+} -HB is 0.0023 (Table 1). Since the complex can be purified by dialysis using a Spectrapor membrane with a molecular weight cut-off of 6000–8000, the degree of polymerization is presumably ≥ 11 . The absorption spectrum of Al^{3+} -HB complex in neutral media does not change markedly on exposure to a 500 W Hg lamp irradiating at 578 nm for 30 min. This indicates that Al^{3+} -HB has a high photochemical stability in neutral media at room temperature. However, at higher temperatures (above 75 °C), the absorption spectrum of Al^{3+} -HB changes significantly. In addition, a preliminary study has demonstrated that Al^{3+} -HA retains the photodynamic action of its parent compound HA, although little quantitative work has been done.^{18–20} Thus it is desirable to investigate the photodynamic properties of Al^{3+} -HB quantitatively here. In the following experiments, we survey the efficiency of the photosensitized generation of active oxygen species by Al^{3+} -HB, as compared to HB.

Generation of superoxide radical anions ($\text{O}_2^{\cdot-}$) by Al^{3+} -HB

EPR spin trapping. When an air-saturated DMSO solution containing Al^{3+} -HB (0.5 mg mL^{-1}) and DMPO (50 mM) was irradiated, an EPR signal appeared immediately (Fig. 5 inset). This EPR spectrum was characterized by three coupling constants, which are due to the nitrogen and two hydrogen atoms at the β and γ positions. The g factor and the constants determined ($g = 2.0056$, $\alpha^{\text{N}} = 12.5 \text{ G}$, $\alpha_{\beta}^{\text{H}} = 10.2 \text{ G}$ and $\alpha_{\gamma}^{\text{H}} = 1.2 \text{ G}$) are in good agreement with literature values for the DMPO-superoxide radical adduct.³⁴

Control experiments confirmed that Al^{3+} -HB, oxygen and light were all necessary for the production of the EPR signal shown in the inset of Fig. 5 (Fig. 5, line 2). The addition of SOD ($30 \mu\text{g mL}^{-1}$) prior to illumination inhibited the EPR signal intensity (Fig. 5, line 3). These observations support the assignment of the EPR spectrum to the DMPO- $\text{O}_2^{\cdot-}$ adduct.

In addition, we compared the $\text{O}_2^{\cdot-}$ -generation efficiency of Al^{3+} -HB with HB on the basis of the same optical density at 578 nm (Fig. 5, line 4). It can be seen that Al^{3+} -HB can readily photosensitize $\text{O}_2^{\cdot-}$ generation, with an efficiency about twice as much as that of HB.

SOD inhibitable cytochrome c reduction. Although the spin trapping method is at least 20 times more sensitive than the reduction of cytochrome c for the measurement of superoxide radical anions, the cytochrome c method appears to be more applicable for the quantitative analysis of $\text{O}_2^{\cdot-}$ relative to DMPO spin trapping.³⁵ Fig. 6 shows the visible absorption spectrum of reduced cytochrome c, produced during the irradiation of an oxygen-saturated solution containing Al^{3+} -HB

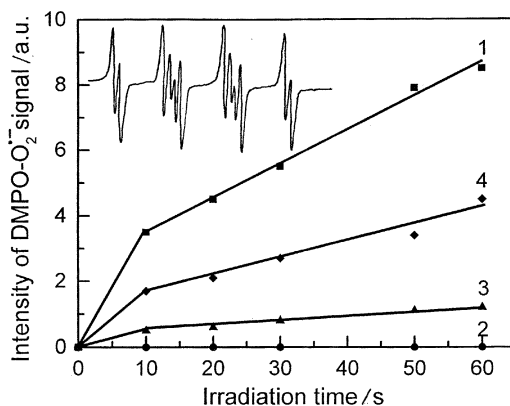
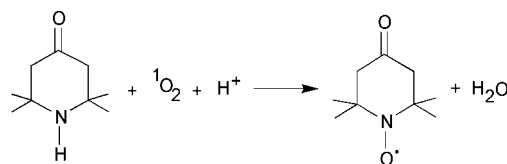


Fig. 5 The dependence of the DMPO-superoxide radical adduct intensity on irradiation time derived from irradiation of an air-saturated DMSO solution containing Al^{3+} -HB (0.5 mg mL^{-1}) and DMPO (50 mM) (line 1). Line 2: same as line 1 except that Al^{3+} -HB, oxygen or illumination was omitted. Line 3: same as line 1 except that SOD ($30 \mu\text{g mL}^{-1}$) was added. Line 4: same as line 1 except that Al^{3+} -HB was replaced by HB. Inset: the EPR signal of DMPO- $\text{O}_2^{\cdot-}$ adducts generated under the same conditions as line 1 (a.u., arbitrary units). Instrumental settings: microwave power, 10 mW; modulation amplitude, 1 G; scan width, 100 G; receive gain, 1.25×10^4 .

(0.05 mg mL^{-1}) and cytochrome c ($85 \mu\text{M}$). The increase in absorbance at 550 nm is characteristic of the reduction of cytochrome c (Cyt Fe^{3+}).^{28,29} Superoxide radical anions may be detected quantitatively by determining the amount of reduced cytochrome c (Cyt Fe^{2+}) produced by $\text{O}_2^{\cdot-}$ that is inhibitable by SOD.^{28,29,31} The rate of $\text{O}_2^{\cdot-}$ generation by Al^{3+} -HB was determined to be about $2.3 \mu\text{M min}^{-1}$ under our experimental conditions.

Photogeneration of singlet oxygen ($^1\text{O}_2$) by Al^{3+} -HB

EPR detection. It has previously been reported that TEMPO, a nitroxide radical detectable by EPR, can be generated from the reaction of TEMP and singlet oxygen [eqn. (1)].³⁷



As shown in the inset of Fig. 7, the EPR spectrum of triplet peaks with equal intensity, characteristic of a nitroxide

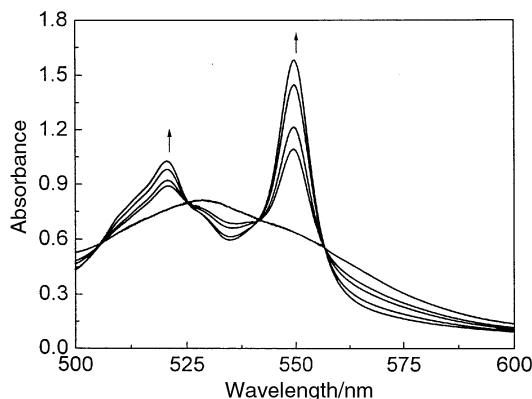


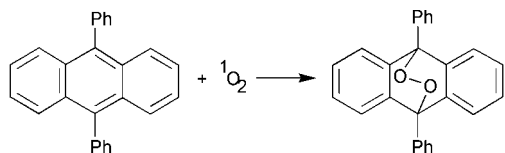
Fig. 6 Absorbance spectra of an oxygen-saturated aqueous solution (pH 7.4) containing Al^{3+} -HB (0.05 mg mL^{-1}) and ferrocyanochrome c ($85 \mu\text{M}$) under different irradiation times: 0, 10, 13, 18, 20 min. In the presence of SOD ($60 \mu\text{g mL}^{-1}$), the spectrum at 0 min was unchanged after 20 min of continuous irradiation.

radical, was observed when an air-saturated DMSO solution of Al^{3+} -HB (0.5 mg mL^{-1}) and TEMP (20 mM) was irradiated at room temperature. This spectrum is comparable with that of commercial TEMPO. The hyperfine splitting constant and g factor of the oxidation product of TEMP photosensitized by Al^{3+} -HB are identical to those of commercial TEMPO ($a^N = 16.3 \text{ G}$, $g = 2.0056$).³⁶ In the absence of Al^{3+} -HB, oxygen or irradiation, no EPR signal could be detected (Fig. 7, line 2). These data demonstrate that the formation of the nitroxide radical is a photodynamic process.

To provide more evidence to support the involvement of $^1\text{O}_2$ in the Al^{3+} -HB photosensitizing process, further experiments were carried out. In the presence of an $^1\text{O}_2$ scavenger (DABCO or NaN_3), the EPR signal was suppressed (Fig. 7, line 3). The effect of deuterated solvent on the yield of TEMPO was also studied. It was found that the intensity of the EPR signal increased approximately three-fold when DMSO was replaced by fully deuterated DMSO as solvent (data not shown). These two powerful tools, both of which are diagnostic for $^1\text{O}_2$, suggest that TEMPO is derived from the reaction of TEMP with $^1\text{O}_2$.

Determination of $^1\text{O}_2$ quantum yield generated by Al^{3+} -HB.

The DPA bleaching method has been confirmed to be an efficient measurement for the quantum yield of $^1\text{O}_2$ generated during photosensitization [eqn. (2)].²⁷



In order to determine the quantum yield of $^1\text{O}_2$ generated by Al^{3+} -HB, we adopted the 9,10-DPA bleaching method with HB as reference. During the measurements, the optical densities at 578 nm of the samples were adjusted to be the same. The absorption spectra of Al^{3+} -HB in the DPA bleaching system after different irradiation times are shown in the inset of Fig. 8. Fig. 8 shows the rates of DPA bleaching photosensitized by Al^{3+} -HB (line 1) and HB (line 2) as a function of irradiation time in DMSO. Control experiments indicate that no DPA bleaching occurs when photosensitizers, oxygen or irradiation are absent (Fig. 8, line 3). The addition of DABCO

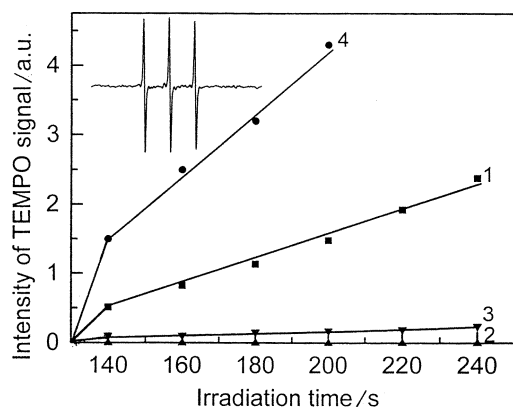


Fig. 7 The EPR signal intensity of TEMPO formed in an air-saturated DMSO solution of Al^{3+} -HB (0.5 mg mL^{-1}) and TEMP (20 mM) as a function of illumination time using 532 nm light (line 1). Line 2: same as line 1 except that Al^{3+} -HB, oxygen or illumination was omitted. Line 3: same as line 1 except that NaN_3 (2 mM) was added. Line 4: same as line 1 except that Al^{3+} -HB was replaced by HB (0.3 mM). The inset shows a typical EPR spectrum of TEMPO formed during irradiation of a solution under the same conditions as line 1. Instrumental settings: microwave power, 10 mW ; modulation amplitude, 1 G ; scan width, 100 G ; receive gain, 1.25×10^4 .

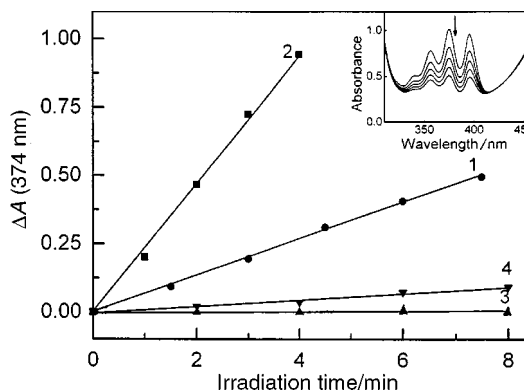


Fig. 8 Photosensitized DPA bleaching by measuring the absorbance decrease (ΔA) at 374 nm as a function of irradiation time in oxygen-saturated DMSO solution containing Al^{3+} -HB (0.08 mg mL^{-1}) and DPA (0.3 mM) (line 1). Line 2: same as line 1 except that Al^{3+} -HB was replaced by HB ($39 \mu\text{M}$). Line 3: same as line 1 except that Al^{3+} -HB, oxygen or light was omitted. Line 4: same as line 1 except that NaN_3 (5 mM) was added. The absorption spectra in the DPA bleaching system upon irradiation for 1.5, 3, 4.5, 6 and 7.5 min. The arrow indicates the direction of change.

or NaN_3 (5 mM) almost completely inhibited DPA bleaching (Fig. 8, line 4). This confirms that the bleaching of DPA results from the reaction of DPA with $^1\text{O}_2$ formed by Al^{3+} -HB photosensitization. The $^1\text{O}_2$ -generating quantum yield for Al^{3+} -HB in DMSO was estimated to be 0.23, relative to HB (0.76). The Al^{3+} -HB photosensitized generation of $^1\text{O}_2$ was also investigated in ethanol, in which the relative quantum yield of $^1\text{O}_2$ for Al^{3+} -HB was found to be 0.22 (HB in ethanol, 0.76). It can be seen that the quantum yield of singlet oxygen changes little in different polar solvents.

Conclusions

In this paper, we report the synthesis of a new photosensitizer, Al^{3+} -HB (3), in high yields. The Al^{3+} -HB complex possesses a polymeric cationic structure similar to Al^{3+} -HA. The absorption of Al^{3+} -HB shifts bathochromically and the water solubility is enhanced significantly compared with HB. The EPR and spectrophotometric measurements demonstrate that the superoxide radical anion ($\text{O}_2^{\cdot-}$) and singlet oxygen ($^1\text{O}_2$) can be produced by Al^{3+} -HB photosensitization. The efficiency of $\text{O}_2^{\cdot-}$ generation by Al^{3+} -HB is about twice as much as that of HB, while the $^1\text{O}_2$ generation efficiency is only one third of that of HB. However, this does not necessarily mean that the photosensitizer possesses less photodynamic efficiency than HB because additional pathways may be involved in the antiviral and anti-tumor activity.³⁷ It is apparent that the Al^{3+} -HB complex might be potentially useful as a phototherapeutic agent, just like the parent hypochlorins.

Acknowledgements

This research was supported by the 95 key project of Academia Sinica (no. KJ952-J1-523) and the National Science Foundation of China (no. 39830090).

References

1. M. Ochsner, *J. Photochem. Photobiol. B*, 1997, **39**, 1.
2. L. J. Jiang, *Chin. Sci. Bull.*, 1990, **21**, 1608.
3. L. J. Jiang, *Chin. Sci. Bull.*, 1990, **21**, 1681.
4. Z. J. Diwu and J. W. Lown, *Photochem. Photobiol.*, 1990, **52**, 609.
5. Z. J. Diwu and J. W. Lown, *Pharmacol. Ther.*, 1994, **63**, 1.
6. J. X. Liu, G. G. Miller, L. R. Huang, Z. J. Diwu, J. W. Lown, J. Tulip and M. S. Mcphee, *J. Labelled Compd. Radiopharm.*, 1995, **XXXVI**, 815.

- 7 G. G. Miller, K. Brown, R. B. Moore, Z. J. Diwu, J. X. Liu, L. R. Huang, J. W. Lown, D. A. Begg, V. Chlumecky, J. Tulip and M. S. Mcphee, *Proc. SPIE Int. Soc. Opt. Eng.*, 1995, **2371**, 97.
- 8 E. P. Estey, K. Brown, Z. J. Diwu, J. X. Liu, J. W. Lown, G. G. Miller, R. B. Moore, J. Tulip and M. S. Mcphee, *Cancer Chemother. Pharmacol.*, 1996, **37**, 343.
- 9 J. B. Hudson, J. Zhou, J. Chen, L. Harris, L. Yip and G. H. N. Towers, *Photochem. Photobiol.*, 1994, **60**, 253.
- 10 J. B. Hudson, V. Imperial, R. P. Haugland and Z. J. Diwu, *Photochem. Photobiol.*, 1997, **65**, 352.
- 11 Y. Z. Hu and L. J. Jiang, *J. Photochem. Photobiol. B*, 1996, **33**, 51.
- 12 Z. J. Diwu, C. L. Zhang and J. W. Lown, *Anti-Cancer Drug Des.*, 1993, **8**, 129.
- 13 Y. Y. He, J. Y. An and L. J. Jiang, *J. Photochem. Photobiol. A*, 1999, **120**, 191.
- 14 Y. Y. He, J. Y. An and L. J. Jiang, *Int. J. Radiat. Biol.*, 1998, **74**, 647.
- 15 Y. Z. Song, J. Y. An and L. J. Jiang, *Biochim. Biophys. Acta*, 1999, **1472**, 307.
- 16 W. G. Zhang, M. Weng, S. Z. Pang, M. H. Zhang, H. Y. Yang, H. X. Zhao and Z. Y. Zhang, *J. Photochem. Photobiol. B*, 1998, **44**, 21.
- 17 Y. Jiang, J. Y. An and L. J. Jiang, *Chin. Sci. Bull.*, 1993, **38**, 797.
- 18 Z. J. Diwu, C. L. Zhang and J. W. Lown, *J. Photochem. Photobiol. A*, 1992, **66**, 99.
- 19 J. Y. An, F. Tian, Y. Z. Hu and L. J. Jiang, *Chin. J. Chem.*, 1993, **11**, 532.
- 20 Y. Z. Hu, J. Y. An and L. J. Jiang, *J. Photochem. Photobiol. B*, 1994, **22**, 219.
- 21 M. H. Zhang, S. Chen, J. Y. An and L. J. Jiang, *Chin. Sci. Bull.*, 1989, **34**, 1008.
- 22 K. H. Zhao and L. J. Jiang, *Chin. J. Org. Chem.*, 1989, **9**, 252.
- 23 Y. Y. He, J. Y. An and L. J. Jiang, *Dyes Pigm.*, 1999, **41**, 79.
- 24 H. Beraldo, A. Garnier-Suillerot and L. Tosi, *Inorg. Chem.*, 1983, **22**, 4117.
- 25 H. B. Singh, J. Sharma and T. S. Rao, *Indian J. Chem Sect. A*, 1987, **26**, 167.
- 26 A. E. Harvey, Jr. and D. L. Manning, *J. Am. Chem. Soc.*, 1950, **72**, 4488.
- 27 Z. J. Diwu and J. W. Lown, *J. Photochem. Photobiol. A*, 1992, **64**, 273.
- 28 I. Fridovich, in *CRC Handbook of Methods for Oxygen Radical Research*, ed. R. A. Greenwald, CRC Press, Boca Raton, FL, 1985, pp. 121–122.
- 29 I. Fridovich, *J. Biol. Chem.*, 1970, **245**, 4053.
- 30 W. F. Beyer and I. Fridovich, *Arch. Biochem. Biophys.*, 1962, **58**, 593.
- 31 C. Hadjur and P. Jardon, *J. Photochem. Photobiol. B*, 1995, **29**, 147.
- 32 C. Hadjur, G. Wagnières, F. Ihringer, Ph. Monnier and H. van den Bergh, *J. Photochem. Photobiol. B*, 1997, **38**, 196.
- 33 C. Hadjur, A. Jeunet and P. Jardon, *J. Photochem. Photobiol. B*, 1994, **26**, 67.
- 34 K. Lang, D. M. Wagnerová, P. Stopka and W. Damerau, *J. Photochem. Photobiol. A*, 1992, **67**, 187.
- 35 S. P. Sanders, S. J. Harrison, P. Kuppusamy, J. T. Sylvester and J. L. Zweier, *Free Radical. Biol. Med.*, 1994, **16**, 753.
- 36 Y. Lion, M. Delmelle and A. van de Vorst, *Nature*, 1976, **263**, 442.
- 37 R. Chaloupka, F. Sureau, E. Kocisova and J. W. Petrich, *Photochem. Photobiol.*, 1998, **68**, 44.